Numerical Simulation of Two-Dimensional Inlet Flowfields

S Biringen*
Old Dominion University, Norfolk Virginia

Inlet flowfields for airbreathing missiles are calculated by a two dimensional computational method A supersonic freestream is assumed to allow the forebody calculation to be uncoupled from the inlet calculation The inlet calculation employs an implicit, time marching, finite difference procedure to solve the Euler equations formulated in body fitted coordinates The method can be used for a flowfield with both subsonic and supersonic regions and is found to converge rapidly for supercritical inlet operation For subcritical inlet operation, however, convergence to steady state is slow

I Introduction

CALCULATION of inlet flowfields is of considerable importance to the efficient design of airbreathing missiles; for example to maximize cowl drag due to spillage at off design conditions These flowfields are very complex due to their mixed hyperbolic elliptic nature the influence of the forebody and viscous effects as well as three dimensionality The complexities of three dimensional viscous inlet flows make their numerical prediction a very difficult task; therefore, calculation of two dimensional inlets is an evolutionary step toward that direction

The present work mainly focuses on the calculation of inviscid inlet flowfields with uniform and nonuniform inflow boundary conditions; viscous effects which can be important to simulate flow reversal and separation are not considered A recently developed code that employs an implicit time marching solution technique[1,2] for numerically solving the time dependent Euler equations for the flow around airfoils is adapted for this purpose The main factors that influence the choice of a time marching implicit procedure usually are the ability to use the same difference operator in both subsonic and supersonic regions of the flowfield as well as the theoretically acquired numerical stability for time steps much larger than those permitted in explicit marching methods A critical assessment of the second factor will be made in Sec III within the framework of the calculations reported herein

The computation of inlet flowfields has been the subject of a number of investigations Explicit time marching finite difference techniques have been used in Refs 3 and 4 to solve the Euler equations and in Ref 5 an explicit solution procedure was used to solve the Navier Stokes equations with the thin layer approximation For these methods it is well known that the Courant Friedrichs Lewy (CFL) stability criterion restricts the allowable time step and hence for finely clustered meshes (e g near solid boundaries where the gradients are very large), convergence rates are very slow In Ref 6 an implicit finite difference method is presented for the solution of the parabolized Navier Stokes equations Note that such methods are limited to supersonic flows and thus cannot be applied to the subcritical case The present work is an attempt to overcome these restrictions by using a time marching implicit scheme Some previous inviscid inlet flowfield calculations using this method were reported in Ref 7 A similar technique is presented in Ref 8 where a simple wedge shaped inlet is calculated using both the Euler equations and the Navier Stokes equations (for laminar flow) with the thin layer approximation

The objectives of this work are twofold The first objective involves a detailed calculation of the flowfield in and about an inlet for a realistic inlet configuration The second objective focuses on a critical assessment of the present calculation procedure from a user s point of view Consideration is given to convergence criteria and the convergence time necessary to obtain solutions All the calculations were performed for the inlet configuration shown in Fig 1 This inlet has a shock on cowl design Mach number of 3 5 and features an initial 5 deg ramp followed by an additional 10 deg isentropic turning The internal surface of the sharp lipped drooped cowl has an initial external angle of 20 deg Finally, a short constant area channel has been added downstream of the duct exit plane to insure uniform outflow This geometry is representative of current design practice and is a very stringent test of the calculation method

II Solution Procedure

The solution procedure employs the Euler equations which are written in conservation law form for two dimensional flows of a perfect gas The general form of the equations for plane flows is given as[2]

$$\partial_t q + \partial_x E + \partial_y F = 0 \tag{1}$$

where

$$q = \begin{bmatrix} \rho \\ \rho u \\ \rho v \\ e \end{bmatrix} \quad E = \begin{bmatrix} \rho u \\ \rho u^2 + p \\ \rho uv \\ u(e+p) \end{bmatrix} \quad F = \begin{bmatrix} \rho v \\ \rho uv \\ \rho v^2 + p \\ v(e+p) \end{bmatrix}$$

In Eq (1) u and v are the velocities along the x and y coordinates respectively p is the pressure ρ the density and e the total energy per unit volume In order to use a body fitted coordinate system the governing equations are rewritten subject to the general transformation

$$\xi = (x\ y\ t) \qquad \eta = (x\ y\ t) \qquad \tau = t \tag{2}$$

Presented as part of Paper 81 0187 at the AIAA 19th Aerospace Sciences Meeting St Louis Mo Jan 12 15 1981; received Aug 15 1982; revision received May 31 1983

*Research Associate Professor; currently Associate Professor of Mechanical Engineering University of New Hampshire Durham N H

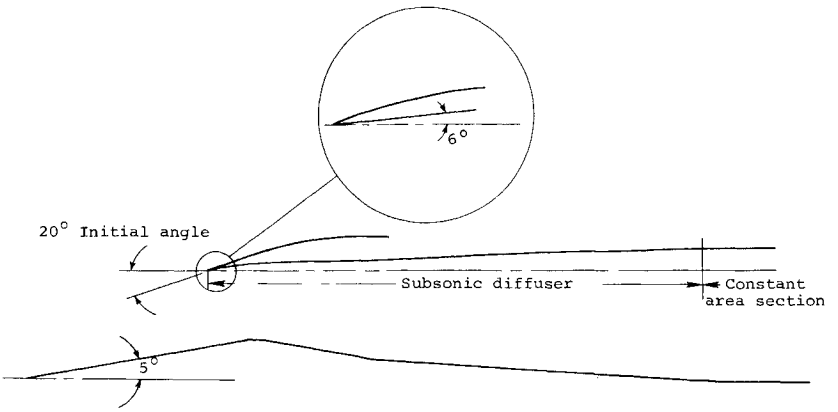

Fig 1 Schematic of inlet geometry, design Mach number of 3 5

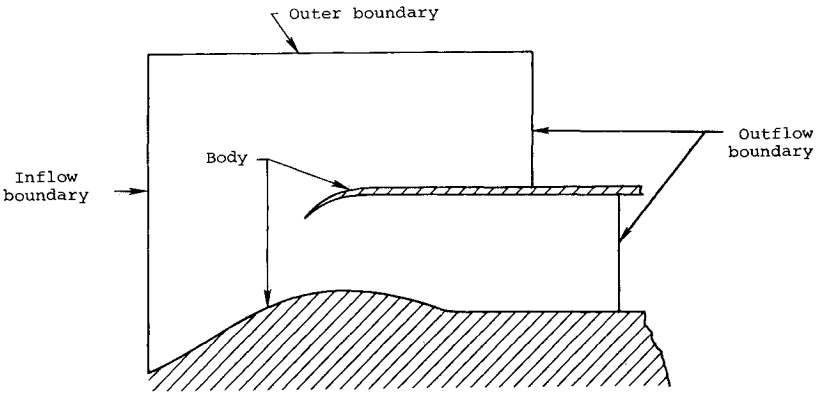

Fig 2 Flowfield boundaries

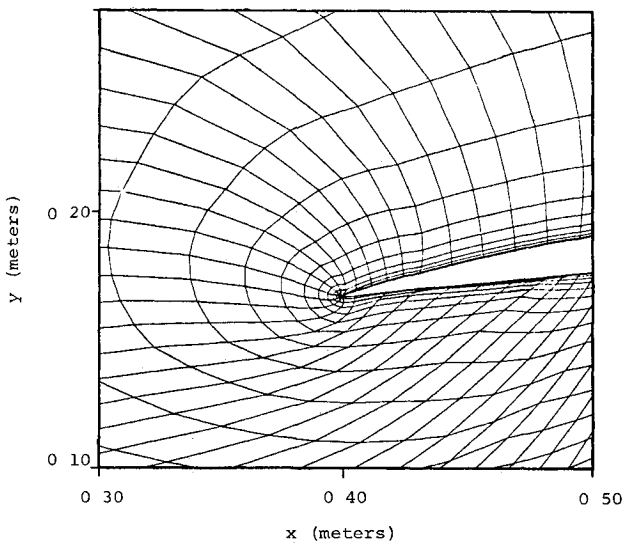

Fig 3 Details of the grid in the vicinity of the cowl tip

where ξ is the coordinate along the body and η is the cross stream coordinate With this approximation, we obtain

$$\partial_\tau \hat{q} + \partial_\xi \hat{E} + \partial_\eta \hat{F} = 0 \tag{3}$$

where

$$\hat{q} = q/J \quad E = (\xi_t q + \xi_x E + \xi_y F)/J$$

$$\hat{F} = (\eta_t q + \eta_x E + \eta_y F)/J$$

and J is the transformation Jacobian Details of the derivation of these equations are available in Ref 2 In the problem under consideration, there are four types of boundaries (Fig 2): solid, inflow outer, and outflow For inviscid calculations, along the cowl and ramp surfaces the tangency condition is satisfied The pressure on the body surface is found from the normal momentum equation; freestream values are specified at the inflow and outer boundaries At the outflow boundary for supercritical inlet conditions all the flowfield variables are calculated by zeroth order extrapolation from the interior For subcritical operation (subsonic duct outflow) extrapolation is used outside the inlet, but at the duct outflow boundary p is set equal to a constant value and v is zero owing to uniform flow conditions at the duct exit Then, in accordance with the equations of continuity and streamwise momentum, u and ρ are calculated by zeroth order extrapolation For uniform outflow these boundary conditions for subcritical operation are consistent with Kentzer's[9] approach used in Ref 8 Initial conditions are specified by using either freestream conditions or the final solution of a previously calculated flowfield

The solution procedure employs a temporal linearization process; the linearized equations are cast into delta form algorithm and the approximate factorization technique is employed [2] The inlet flowfield is obtained as the asymptotic steady state solution of the time marching method

The main advantage of using the governing equations in transformed form is that a body fitted coordinate system in the physical plane can be mapped onto a rectangular coor dinate system in the computational plane Moreover grid points can be clustered in regions where large gradients of the flowfield variables are expected to occur In this work the computer code of Ref 10 that generates body fitted coor dinates for airfoils was modified and used for the inlet geometry An exponential clustering transformation was employed which clusters grid points near each surface along the η direction

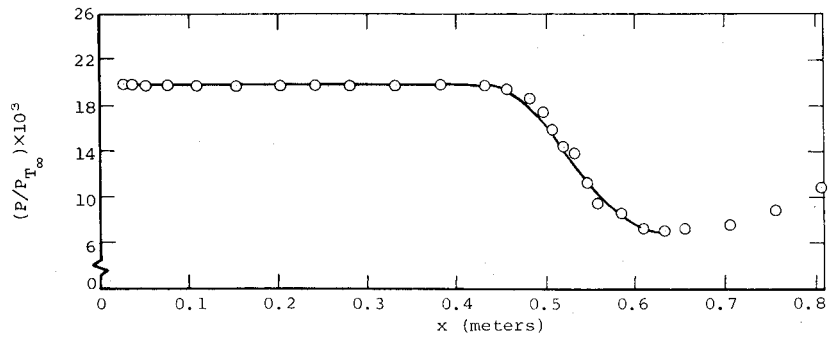

Fig. 4 Pressure distribution on ramp surface, supercritical flow: o, computation; —, shock expansion theory.

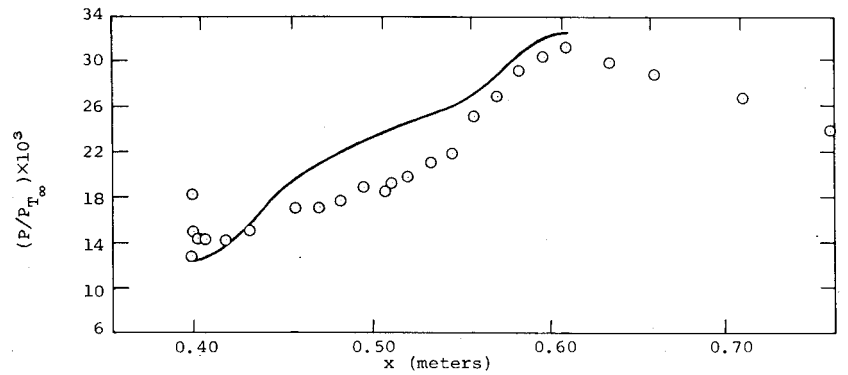

Fig. 5 Pressure distribution on cowl inner surface, supercritical flow: o, computation; —, shock expansion theory.

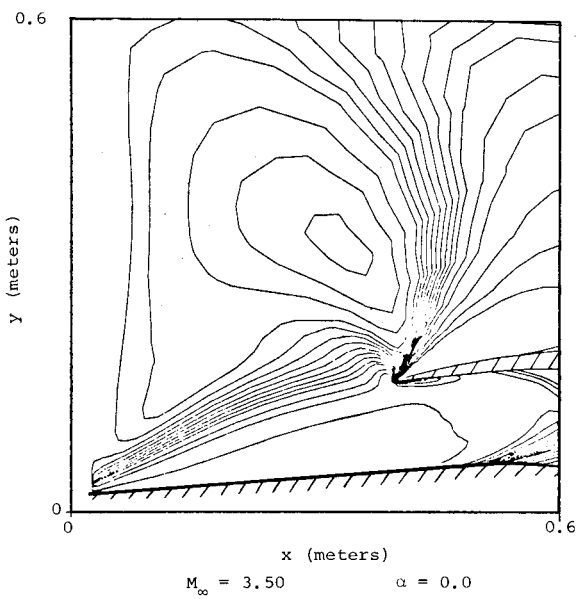

Fig. 6 Details of pressure contours in the vicinity of the cowl tip, supercritical case.

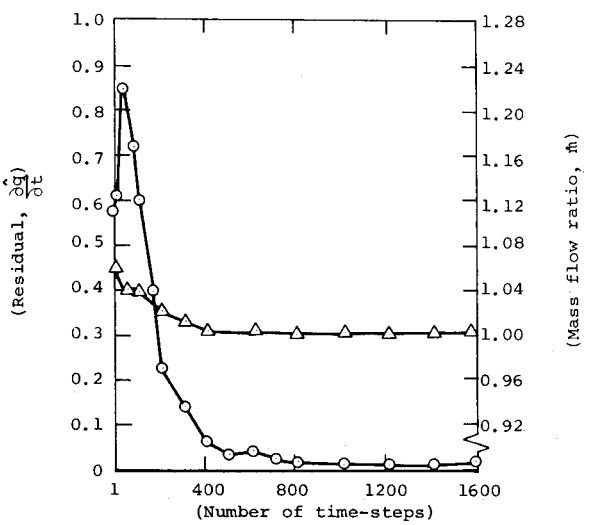

Fig. 7 Rate of convergence of the supercritical solution: o, the residual; Δ, $\dot{m}$, mass flow ratio.

III. Results

In this section, results are presented and discussed for calculations involving supercritical and subcritical inlet operation with uniform inflow boundary conditions and supercritical operation with nonuniform inflow boundary conditions. All the calculations were performed at the design Mach number of the inlet, $M_\infty = 3.5$, using a grid with 72 nodes along ξ and 36 nodes along the η direction. Figure 3 displays the grid in the vicinity of the cowl tip where it is well clustered to capture the rapid variations of the flowfield variables in this region. The grid is coarse in the external flowfield far from the cowl because this area is not important for our present purposes. The outer boundary of the grid was chosen in order to include the bow shock from the forebody in the case of calculations using nonuniform initial conditions.

Results from calculations with supercritical outflow boundary conditions are shown in Figs. 4-7; in this case, the flow is completely supersonic. In Fig. 4 the ramp surface pressure distributions are compared with values obtained using two-dimensional shock expansion theory and Prandtl-Meyer turning analysis; good agreement is shown. Figure 5 displays a similar comparison for the surface pressure distribution on the initial portion of the cowl inner surface. Except in the immediate vicinity of the cowl tip, fair comparison is shown, although the calculated results remain somewhat lower. The discrepancy at the cowl tip is likely due to a combination of a singularity introduced by the very sharp cowl tip and the smearing caused by the shock-capturing process. Figure 6 shows the details of the pressure contours around the cowl tip indicating the existence of a complicated

system of shock waves and expansion waves In particular the initial ramp shock and the shock at the cowl tip are clearly depicted; the occurrence of some shock smearing due to the calculation procedure is also present in this figure Finally, the effects of the coarse grid are evident in the flowfield calculated outside the ramp shock

In Fig 7 convergence history of the calculations for this case are detailed In estimating the progression of the solution to convergence we have examined the time behavior of the residual $\partial\hat{q}/\partial t$ and the mass flow ratio $\dot{m}$ The behavior of these quantities (Fig 7) indicates that the solution has con verged in about 800 1000 time steps As expected the value of $\dot{m}$ reaches unity as the solution converges; in the converged solution, the section to section variation of $\dot{m}$ was less than 1% The calculation takes about 0 75 s of CPU time per time step on the CDC 7600 computer at NASA/ARC and the total CPU time spent on a typical supercritical flow solution is about 500 750 s

The converged solution described above was used to initiate a subcritical calculation to test the capabilities of the method for this more difficult case The back pressure at the duct outflow boundary was set to a value high enough to insure subsonic outflow namely, $P_B = 0\ 7P_{T_\infty}$ and the value of P_B was slowly increased to its full value over about 200 time steps thus simulating a time dependent boundary condition [8]

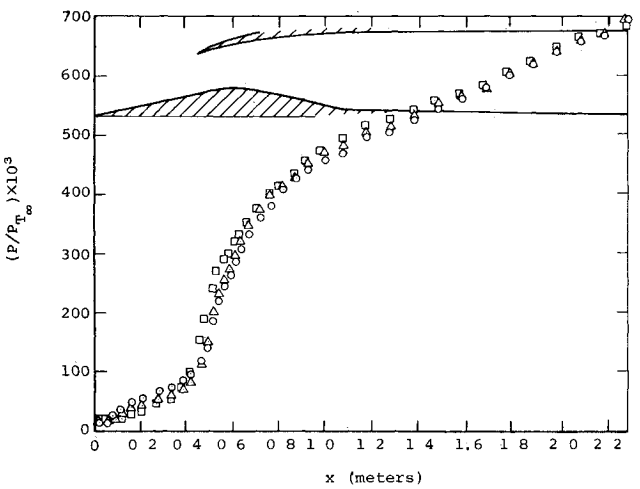

Fig 8 Pressure distribution on ramp surface for subcritical solution with $P_B/P_{T_\infty} = 0\ 7$: o denotes 7500 time steps; Δ denotes 8000 time steps; □ denotes 8500 time steps

At the duct outflow plane the subcritical inlet operation is characterized by the formation of a compression wave which travels upstream and forms a strong shock wave at the inlet throat During the integration process we found that once the shock reaches the ramp the time step had to be reduced to insure the Courant number (CN) to be less than unity for numerical stability to obtain a solution with the shock ex pelled from the inlet For the flowfield equations employed here the Courant number is defined[2] as $\mathrm{CN} \equiv (\Delta t/\Delta\xi)(\tau_{\hat{A}}$ or $\tau_{\hat{B}})$ where $\tau_{\hat{A}}$ or $\tau_{\hat{B}}$ is the maximum spectral radius of the local eigenvalues of $\hat{A}$ or $\hat{B}$ and $\hat{A} \equiv \partial\hat{E}/\partial\hat{q}$ and $\hat{B} \equiv \partial\hat{F}/\partial t$ The reasons for the necessity of decreasing the Courant number can be explained by considering the eigenvalues of $\hat{A}$ which are given as[2]

$$\lambda_{1-4} = U\ U\ U \pm c\sqrt{\xi_x^2 + \xi_y^2}$$

where c is the speed of sound and ξ_x and ξ_y are the metric coefficients of the coordinate transformation In the sub critical case the increased speed of sound behind the shock in the subsonic region (coupled with very large values of the metric coefficients in the vicinity of the ramp where the mesh is finely clustered along both ξ and η) increases the magnitude of the local eigenvalue $U + c\sqrt{\xi_x^2 + \xi_y^2}$ thus making the problem locally very stiff Accordingly, for subcritical inlet operation the present implicit technique does not seem to offer any marked advantage over explicit solution techniques For this case a special "pressure smoothing" which consists of averaging the pressure by adjacent values after each time step, was also applied for numerical stability purposes

In Figs 8 and 9, surface pressure distributions for the subcritical case are shown for three instants in time after the pressure smoothing operator was turned off except in the very close vicinity of the cowl In Fig. 8 the pressure distribution on the ramp surface at 8500 time steps shows a shock structure that is less smeared and steeper than the one at 7500; also note that the normal shock has moved upstream with increasing time steps This lends support to the idea that the solution will improve further with increasing time steps. Pressure distributions on the cowl inner surface (Fig 9) reveals a similar behavior Density contours for this case are shown in Fig. 10 at 8500 time steps in which the terminal shock at the cowl tip is depicted It should be noted that even after 8500 time steps the normal shock is smeared over a fairly large number of grid points

Convergence history of the solution for this case is shown in Fig 11 Each sharp increase in the residual corresponds to a change in the calculation input; that is, decreases of Courant number or a local application of the smoothing operator The

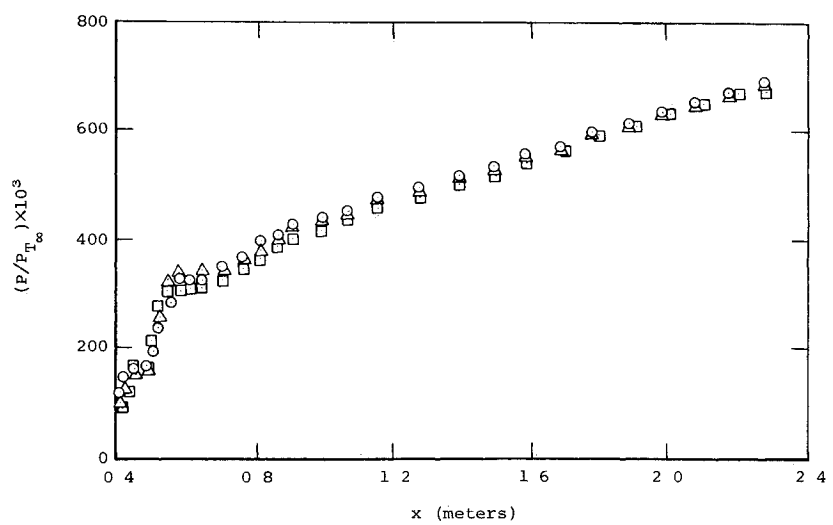

Fig 9 Pressure distribution on cowl inner surface for subcritical solution with $P_B/P_{T_\infty} = 0\ 7$ o denotes 7500 time steps; Δ denotes 8000 time steps; □ denotes 8500 time steps

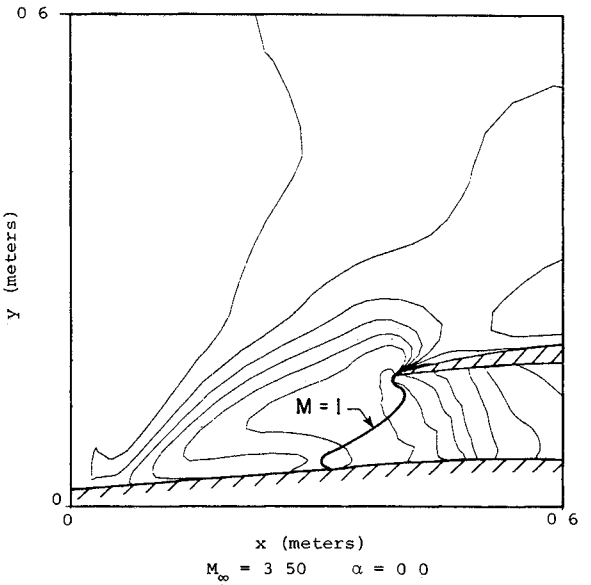

Fig 10 Details of density contours, subcritical case

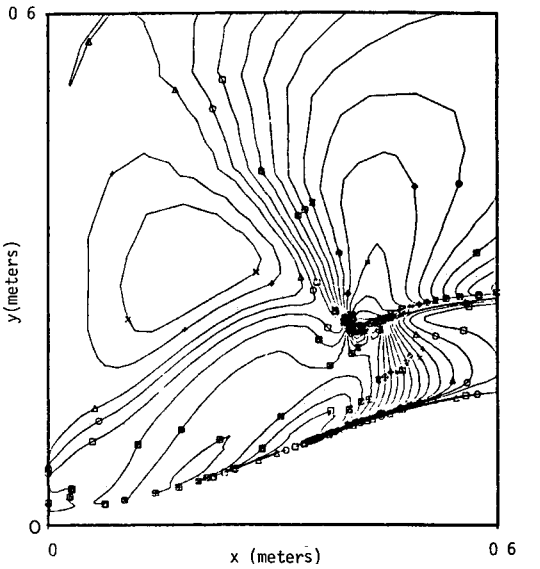

Fig 12 Details of Mach contours subcritical case with the 56×30 grid [7]

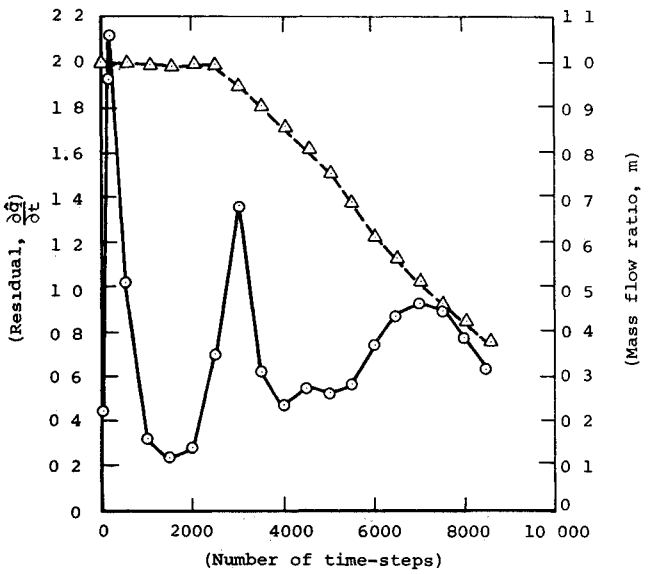

Fig 11 Rate of convergence of the subcritical solution: o, residual; Δ $\dot{m}$ mass flow ratio

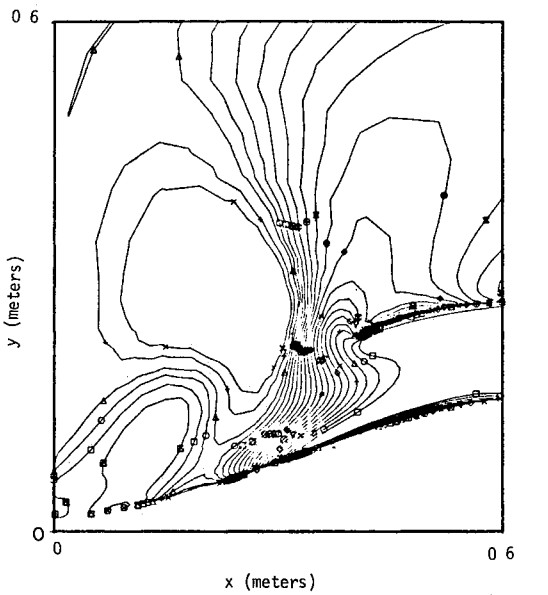

Fig 13 Details of Mach contours, subcritical case with the 56×30 grid[7] with the normal shock expelled from the inlet

trends displayed by both the residual and $\dot{m}$ show that even at 8500 time steps the calculation is not yet converged Hence it is our estimate that a much larger number of time steps will be required to obtain convergence

Although we have not run this subcritical case to con vergence, we demonstrated in Ref 7 that eventually a con verged solution for subcritical operation can be obtained In Figs 12 and 13, we present the final solution for a subcritical case calculated for a similar inlet geometry on a 56×30 grid from Ref 7 Mach contours shown in these figures clearly display the normal shock moving upstream and forming a terminal shock expelled from the inlet. Although these calculations demonstrated the ability of the method to obtain a subcritical solution, convergence time for this case was also very long due to time step restrictions for numerical stability

The capability of the method to calculate a realistic situation in which the inlet is immersed in the flowfield produced by a forebody was tested by using nonuniform inflow boundary conditions To this end the method of Ref 11 was used to generate a solution at $M_\infty = 3\ 5$ and at zero angle of attack for a forebody consisting of a 2 46 caliber von Kármán ogive nose coupled to a cylindrical section This method involves the integration of the three dimensional Euler equations by a space marching technique and is well tested and documented elsewhere [11] In the present calculations, the ratio of body diameter to inlet capture height was taken equal to three which is representative of a realistic configuration The solution at $x/D = 45$ was used as the in flow boundary condition for the inlet calculation on this boundary Results for calculations with supercritical outflow boundary conditions are shown in Figs 14 16 In Fig 14 surface pressure distributions on the ramp and in Fig 15 surface pressure distributions on the cowl inner surface are compared with the results from the calculations with uniform initial conditions As expected, surface pressures from this case are significantly higher due to the presence of the forebody shock although the general trends displayed by both calculations are similar

Details of the convergence history for this calculation are given in Fig 16 These indicate that the solution converges in

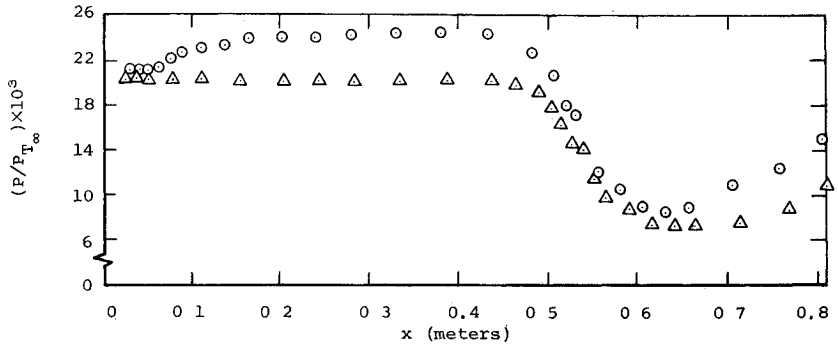

Fig 14 Pressure distribution on ramp surface, supercritical flow: o, nonuniform initial con ditions; Δ, uniform initial conditions

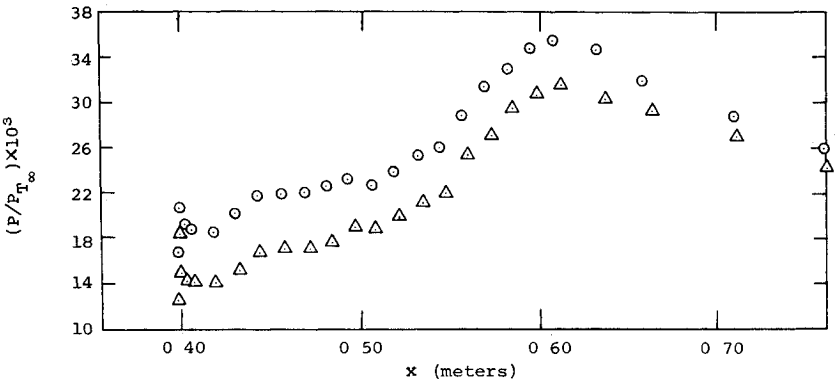

Fig 15 Pressure distribution on cowl inner sur face o denotes nonuniform initial conditions; Δ denotes uniform initial conditions

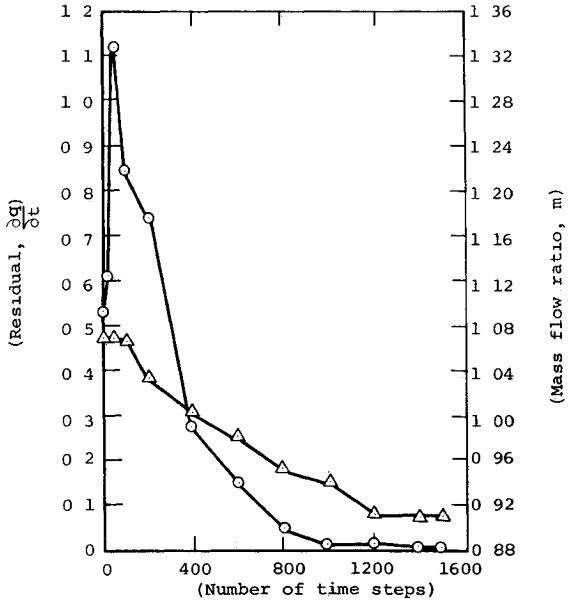

Fig 16 Rate of convergence of the supercritical solution with nonuniform initial conditions: o the residual; Δ $\dot{m}$ the mass flow ratio

about 1500 time steps and that the mass flow ratio is about 8% less than the mass flow ratio obtained with uniform initial conditions Note that U_∞ is used to calculate $\dot{m}$ in all cases

IV Concluding Remarks

A time implicit finite difference solution procedure for the Euler equations has been applied to the calculation of two dimensional inlet flowfields Results for a practical inlet configuration are presented For supercritical operation with uniform and nonuniform inflow conditions solutions converge rapidly; however the accuracy of the method under these conditions awaits experimental evaluation Calculations performed for subcritical inlet operation indicated that for this case the solution converges very slowly The necessity of using very small steps for numerical stability (once the shock reaches the throat) is the main contributing factor

Acknowledgments

This work was supported by NASA Langley Research Center under Contract NAS1 15951 to Nielsen Engineering and Research, Inc Mountain View California

References

[1] Beam R and Warming R F An Implicit Finite Difference Algorithm for Hyperbolic Systems in Conservation Law Form *Journal of Computational Physics* Vol 22 Sept 1976 pp 87 100

[2] Steger J L Implicit Finite Difference Simulation of Flow About Arbitrary Geometries With Application to Airfoils AIAA Paper 77 665 June 1977

[3] D Souza N , Molder, S and Moretti G Numerical Method for Hyperbolic Internal Flow Over Blunt Leading Edges and Two Blunt Bodies *AIAA Journal* Vol 10 May 1972 pp 617 627

[4] Bansod P Supersonic Flow About Ducted Bodies With Subsonic Internal Boundaries *AIAA Journal* Vol 12 June 1975 pp. 531 538

[5] Knight D D Numerical Simulation of Realistic High Speed Inlets Using the Navier Stokes Equations *AIAA Journal* Vol 15 Nov 1977 pp 1583 1589

[6] Buggeln R C McDonald H Levy, R and Kreskovsky J P Development of a 3 D Supersonic Inlet Flow Analysis NASA CR 3218 Jan 1980

[7] Biringen S. Chaussee D S and McMillan O J , 'Calculation of Inlet Flow Fields by an Implicit Technique ' AIAA Paper 80 0031 Jan 1980

[8] Chaussee D S and Pulliam T H Inlet Simulation Using a Diagonal Implicit Algorithm *AIAA Journal,* Vol 19 Feb 1981 pp. 153 159

[9] Kentzer C P Discretization of Boundary Conditions on Moving Discontinuities *Proceedings of Second International Conference on Numerical Methods in Fluid Dynamics* University of California Berkeley Calif Sept 1970 pp 108 113

[10] Sorenson R L and Steger J L , Simplified Clustering of Nonorthogonal Grids Generated by Elliptic Partial Differential Equations NASA TM 73252 Aug 1977

[11] Kutler P Lomax, H and Warming, R. F , Computation of Space Shuttle Flow Fields Using Noncentered Finite Difference Schemes *AIAA Journal* Vol 11 Feb 1973 pp 196 204